

Efficient Degradation and Expression Prioritization with Small RNAs

Namiko Mitarai^{1,2}, Anna M. C. Andersson¹,
Sandeep Krishna¹, Szabolcs Semsey^{1,3}, and Kim Sneppen¹

¹ Niels Bohr Institute, Blegdamsvej 17, DK-2100, Copenhagen, Denmark.

²Department of Physics, Kyushu University 33, Fukuoka 812-8581, Japan.

³Department of Genetics, Eotvos Lorand University, Budapest H-1117, Hungary.

E-mail: namiko@stat.phys.kyushu-u.ac.jp

Abstract. We build a simple model for feedback systems involving small RNA (sRNA) molecules based on the iron metabolism system in the bacterium *E. coli*, and compare it with the corresponding system in *H. pylori* which uses purely transcriptional regulation. This reveals several unique features of sRNA based regulation that could be exploited by cells. Firstly, we show that sRNA regulation can maintain a smaller turnover of target mRNAs than transcriptional regulation, without sacrificing the speed of response to external shocks. Secondly, we propose that a single sRNA can prioritize the usage of different target mRNAs. This suggests that sRNA regulation would be more common in more complex systems which need to co-regulate many mRNAs efficiently.

Keywords: RNA interference, small RNA, micro RNA, RyhB, Hfq, feedback

PACS numbers: 87.80.Vt, 87.16.Ac, 89.75.-k, 89.75.Fb

Submitted to: *Phys. Biol.*

1. Introduction

Small noncoding RNAs (sRNAs) have recently been discovered as key components of genetic regulation in systems ranging from bacteria to mammals [1, 2, 3], and this has spurred much activity in understanding their functional advantages. For example, degradation of sRNA with their target mRNAs has been proposed as a mechanism to obtain ultrasensitivity [4].

One particular system which has been extensively studied is the Fe-Fur system in the bacterium *Escherichia coli* which contains the regulatory sRNA RyhB [5, 6]. This system is responsible for maintaining homeostasis of Fe⁺⁺ ions, which are essential for cell functioning but also poisonous at high concentrations. During aerobic exponential growth, iron-using enzymes in *E. coli* utilize around 10⁶ Fe atoms per cell generation, but more than 10⁴ Fe⁺⁺ ions in free or loosely-bound form is poisonous [7, 8]. Thus, the

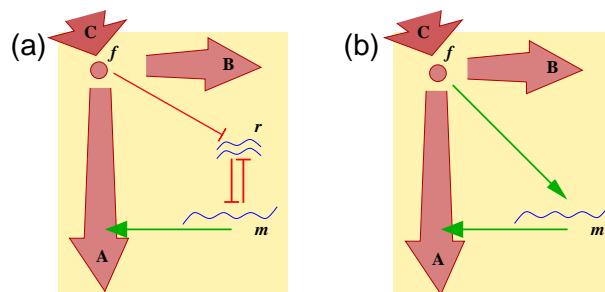


Figure 1. (a) The sRNA motif found in *E. coli*, consists of three variables, f , the Fe-Fur complex which depends on the amount of loosely bound iron, r , the sRNA ryhB, and m , the mRNA of iron-using proteins. The red barred arrows between r and m represent the formation of the $r - m$ complex and its subsequent degradation. The other red barred arrow indicates transcriptional repression of r by f . The influx of f , denoted by C , is divided into the channel A , regulated by m (green arrow), and the non-regulated channel B . (b) The transcription motif found in *H. pylori*. Here, m is transcriptionally activated by f .

cell faces the problem of maintaining a huge flux of Fe through a small reservoir, and at the same time channeling this flux into its most essential functions when the cell is starved of iron: It needs to prioritize and sort the usage of a limited resource.

Reference [9] describes a detailed model of the Fe regulation in *E. coli*, which incorporates several feedback mechanisms that together secure the system against both up and down shifts of the iron level. In this paper, we focus on the prioritization of the usage of iron by the sRNA regulation and its role in sudden iron depletion. The model in [9] is simplified into a core “motif” (Figure 1a) describing the negative feedback used in iron homeostasis. The motif consists of three variables, f the iron-activated Fur (Ferric uptake regulator) protein complex that senses the Fe^{++} level, r , the sRNA RyhB, and m , the mRNA of iron-using proteins. The sRNA works by binding strongly to the mRNA, after which this entire complex is rapidly degraded [10, 11, 12]. The sRNA is in turn transcriptionally repressed by f . Thus, f effectively activates m , through a double negative link via the sRNA.

Interestingly, the regulation of iron homeostasis in the bacterium *Helicobacter pylori* differs from that of *E. coli* in one important respect: the regulation via the sRNA RyhB is replaced by a direct transcriptional activation of the mRNA m by f (see Figure 1b) [13, 14]. These two bacteria motivate us to compare the “sRNA motif” with the corresponding “transcription motif”.

By studying these motifs, we demonstrate the following interesting aspects of sRNA regulation: (i) both motifs can be adjusted to have similar response times, but the metabolic cost is different for the two motifs. (ii) a single type of sRNA can efficiently prioritize expression level of various downstream target mRNAs, thus prioritizing the usage of a limiting resource. We also discuss possible experiments to test these results.

2. The Two Motifs

2.1. sRNA motif

In the motif of Figure 1a we focus on the case where sRNA binds to mRNA and both RNAs in the complex are degraded. In terms of an effective rate constant for the overall degradation, δ , the dynamics of the concentrations of the sRNA (r) and its target mRNA (m) can be described by

$$\frac{dr}{dt} = \alpha_r - \frac{r}{\tau_r} - \delta \cdot r \cdot m \quad (1)$$

$$\frac{dm}{dt} = \alpha_m - \frac{m}{\tau_{mrna}} - \delta \cdot r \cdot m \quad (2)$$

where α_r and α_m set the respective production rates, and τ_r and τ_m define the background degradation times. We next rescale the parameters by measuring concentrations in units of $\alpha_m \tau_r$ and measuring time in units of τ_r ‡.

To these rescaled equations we also add an equation for f , a small-molecule-activated transcription factor for the sRNA (as shown in Figure 1a). We simplify this two step reaction from f to regulation by assuming that all bindings are first order, and by rescaling binding constants such that $f = 1$ results in half-repression of the promoter of the sRNA gene. Including the import and consumption of f in analogy to the Fe-Fur system[9], the full dynamics of the motif becomes:

$$\frac{df}{dt} = \begin{cases} C - A \cdot m - B \cdot f & \text{when } f > 0, \\ C & \text{when } f = 0, \end{cases} \quad (3)$$

$$\frac{dr}{dt} = \frac{\alpha}{1+f} - r - \gamma r \cdot m, \quad (4)$$

$$\frac{dm}{dt} = 1 - \frac{m}{\tau_m} - \gamma r \cdot m. \quad (5)$$

Here the dimensionless mRNA degradation time $\tau_m = \tau_{mrna}/\tau_r$, and the dimensionless degradation rate of the RNAs is related to the dimensionfull parameters as follows:

$$\gamma = \delta \alpha_m \tau_r^2. \quad (6)$$

In the absence of m , r is degraded relatively slowly because unbound sRNA are quite stable *in vivo* [11]. This means that τ_r , which is our rescaled time unit in eqs. (3)-(5), is around (25/ln2) min. In the absence of r , m is degraded with $\tau_m = 0.2$, the lifetime of RyhB target mRNA in *E. coli* from ref. [11].

The most important parameters that determine the dynamics of sRNA regulation are α and γ in eqs.(4) and (5). We can determine a reasonable range of values for these two parameters using experimental data. First, for the Fe-Fur system α and γ are mutually constrained by the observation that the target mRNA, *sodB*, is depleted

‡ The equation are formally rescaled by replacing $m \rightarrow m/(\alpha_m \tau_r)$, $r \rightarrow r/(\alpha_m \tau_r)$ and $t \rightarrow t/\tau_r$. Thereby, a unit of time corresponds to the degradation time of the sRNA, and the unit of production rates corresponds to the production rate of the target mRNA.

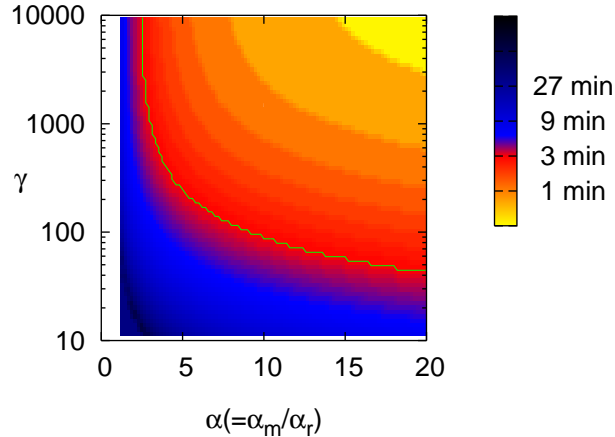


Figure 2. Limits on rescaled sRNA-target mRNA coupled degradation rate $\gamma = \delta\alpha_m\tau_r^2$. The colour shading indicate that the model takes longer (shorter) time in a darker (yellow) region to be depleted 5-fold after the small RNA is activated by setting f from 40 to zero at $t = 0$. The green solid line shows the contour line of 3 min. When production of mRNA is much faster than production of sRNA the 5-fold reduction can be obtained by a small γ , whereas a relatively small $\alpha = \alpha_m/\alpha_r$ makes production of sRNA so slow that the mutual degradation must be very fast. The response time is calculated based on the degradation time of sRNA $\tau_r = (25/\ln 2)\text{min}$ [9].

around 5-fold within 3 minutes after full induction of the RyhB promoter[11]. These 3 minutes include the time required for RyhB production, set by α , plus the time for the produced RyhB to bind to sodB message and to degrade the complex, set by γ . For $\alpha < 1$ there will never be enough RyhB to deplete the message completely, whereas for α slightly higher than 1 an extremely high γ is needed for efficient depletion.

Fig. 2 illustrates this. We simulate eqs. (4) and (5) to measure how long it takes for m to be depleted 5-fold after fully-activating sRNA at $t = 0$ by changing f manually from 40 to zero. The solid line in Fig. 2 shows values of γ and α that give a 3 minutes depletion-time for sodB mRNA. With α values in the range from 3 to 10, we see that physiological γ values would need to be between 100 and 10000. In addition, the reduction of iron consumption occurs as soon as the sRNA-mRNA complex is formed, even before the mRNA is degraded, but the measurement of [11] does not distinguish RNA species in complexes from the free form. Thus, the effective γ could be larger than the above estimate. The value of α can be estimated from other data in ref. [11] of RyhB and sodB time series after induction and repression of RyhB. From these data, we estimate that α is between 2 and 5. In the rest of the paper, we explore the small RNA motif for a range of α and γ values, around the estimates made above.

The three other parameters, A , B , and C , in the iron flux equation (3), we set using experimental data [9], as described in the appendix.

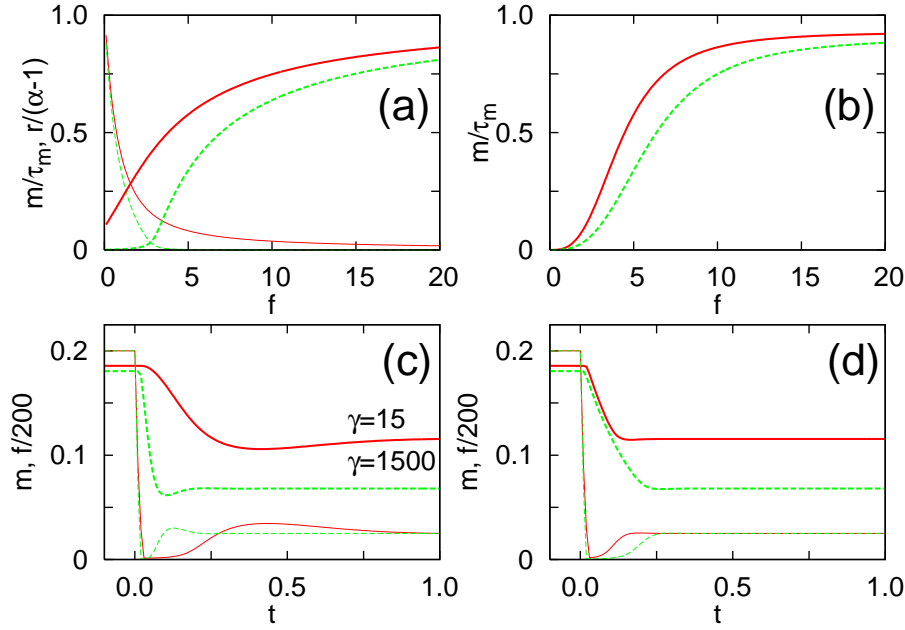


Figure 3. (a) The steady state level of $r/(\alpha - 1)$ (thin lines) and m/τ_m (thick solid lines) vs. f for $\alpha = 4$ with $\gamma = 15$ (red solid lines) and $\gamma = 1500$ (green dashed lines) in the sRNA motif. (b) The steady state level of m/τ_m (thick lines) vs. f for the corresponding transcription motif parameters (see text). The time evolution of f (divided by 200, thin lines) and m (thick lines) for the systems in (a) and (b) are shown in (c) and (d), respectively, after the sudden drop of C at $t = 0$.

2.2. Transcriptional motif

To model the transcription motif (Figure 1b) we replace (4) and (5) by the single equation:

$$\frac{dm}{dt} = D \cdot \frac{f^h}{f^h + K_t^h} - \frac{m}{\tau_m}. \quad (7)$$

The first term models the direct transcriptional activation of m production by f , where D sets the maximum production rate of m and K_t sets the binding constant between f and the DNA. The ‘‘Hill coefficient’’ h sets the steepness of the response, and is related to the cooperativity in binding. We use the same values of the influx C and two constants A and B in (3) as those used in the sRNA motif. We choose D and K_t in the transcription motif to have the identical steady state values of the f and m to the corresponding sRNA motif (parameterized by α and γ) for high iron ($f = 40$) and low iron ($f = 5$). It is not obvious that this is possible for all values of α and γ . In fact, we found that it is not possible for $h \leq 2$, but when $h = 3$, we can set D and K_t such that the above conditions are fulfilled for $\alpha \in [0, 20]$ and $\gamma \in [0, 2000]$. Therefore, henceforth we keep $h = 3$.

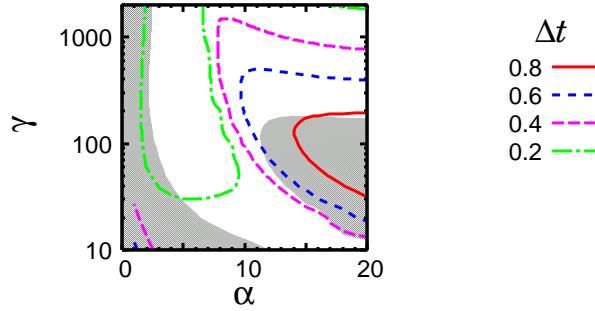


Figure 4. The contour plot of sRNA motif response time, Δt , at which f recovers to and subsequently remains within 95% of the final steady state value. The corresponding transcription motif systems show a faster response in the shaded region.

3. Results

3.1. Degradation times

Figures 3a and b show how the steady state values of r and m depend on the steady state f level, in the sRNA motif for two different γ values, and, respectively, in the corresponding transcription motif systems. For the sRNA motif, a larger γ results in a much larger ratio between maximum and minimum m values, and a steeper drop between them (Figures 3a). This is expected because in the $\gamma \rightarrow \infty$ limit, $m = \max(O(1/\gamma), \tau_m[1 - \alpha/(1 + f)])$, and this steepness in the sRNA regulation is referred to as “ultrasensitivity” in [4]. For the transcription motif, on the other hand, the dependence of m on f is weaker and nearly unaffected by the corresponding change in D and K_t (Figure 3b). This is because the steepness of the curve in the transcription motif is determined by the Hill coefficient h , which is set to be relatively high value 3 but still not enough to give as sharp slope as the sRNA motif with $\gamma = 1500$.

The importance of γ is also evident in the dynamical response of the motifs to a sudden depletion in the external iron source C (Figures 3c and d). For the sRNA motif, Figure 3c shows that a larger γ results in a faster drop in m level, and a quicker approach to the new steady state level. The same is true for the f level also. That is, a large γ naturally ensures a faster removal of all excess m , while also allowing f and m to climb back to non-zero steady levels even after f drops almost to zero during the initial shock. In contrast, the transcription motif displays approximately the same timescale of mRNA drop for the two corresponding cases because a drop in m takes a time proportional to τ_m , independent of other parameters.

We investigate this further by quantifying the response time. Looking at Figure 3c, we see that the f level drops very sharply and then rises towards its final steady state value. During this rise, at some time, Δt , f reaches within 95% of the final steady state value. We use Δt as a measure of the response speed of the system. In Figure 4 we show a contour plot of Δt for a range of values of α and γ . The corresponding transcription motif systems show a faster response than the sRNA motif in the shaded

region. The comparison indicates that sRNA based translational regulation produces a faster response than transcriptional regulation when $\alpha \gtrsim 2$ (and α is not too large compared to the investigated range of f) and γ is larger than a critical level, around 150 (the unshaded region in Figure 4).

3.2. Metabolic cost

The relatively slow response of the transcription motif is, of course, because its response timescale is set by τ_m , which we keep constant. We emphasize that it is possible to achieve a fast response in the transcription motif also by decreasing τ_m . There are some costs associated with this alternative strategy though. Faster mRNA turnover due to lower τ_m requires a higher production to maintain the same homeostatic levels of f . At high f levels, where mRNA is high, the sRNA motif secures a low degradation rate of mRNA, whereas the transcription motif produces the mRNA at its maximum rate. On the other hand, at low f the sRNA motif maintains a high rate of mRNA degradation, while the transcription motif saves resources by reducing mRNA production. Therefore, for a given response speed to sudden iron starvation, the sRNA motif is less costly if the bacterium usually lives in iron-rich conditions, whereas the transcription motif is preferable if the organism mostly lives in iron-poor conditions.

3.3. sRNA prioritize downstream protein levels

3.3.1. Prioritization in the iron feedback motif The properties of sRNA regulation can be used in an interesting way when more than one kind of mRNA is under regulation [12]. Different mRNA can have hugely different binding strengths to the regulating sRNA, and thereby very different effective degradation timescales. This is because the binding strength of the r - m complex is, to a first approximation, an exponential function of the number of matching base-pairs, which can vary by an order of magnitude across different mRNA: The free-energy gain per matching base-pair is around 1 to 2 kcal/mol, which can give the difference in statistical weight $\exp(\Delta G/k_B T) \approx 5$ to 30. Because of this property, sRNA regulation could be used to prioritize the degradation of different mRNA. We illustrate this by adding a second mRNA to the sRNA motif:

$$\frac{dr}{dt} = \frac{\alpha}{1+f} - r - r \cdot (\gamma_1 m_1 + \gamma_2 m_2) \quad (8)$$

$$\frac{dm_1}{dt} = \alpha_{m_1} - \frac{m_1}{\tau_m} - \gamma_1 r m_1, \quad (9)$$

$$\frac{dm_2}{dt} = \alpha_{m_2} - \frac{m_2}{\tau_m} - \gamma_2 r m_2. \quad (10)$$

For f , we use (3), replacing m by $(m_1 + m_2)$. The two mRNAs, m_1 and m_2 , have different effective degradation rates, γ_1 and γ_2 , resulting in different steady state levels for a given C value. Other parameters are set as in the case with a single mRNA. Figure 5 shows the behavior of this system. The steady state level in Figure 5a shows that m_2 , the mRNA with larger γ , is suppressed more than m_1 on depletion of f .

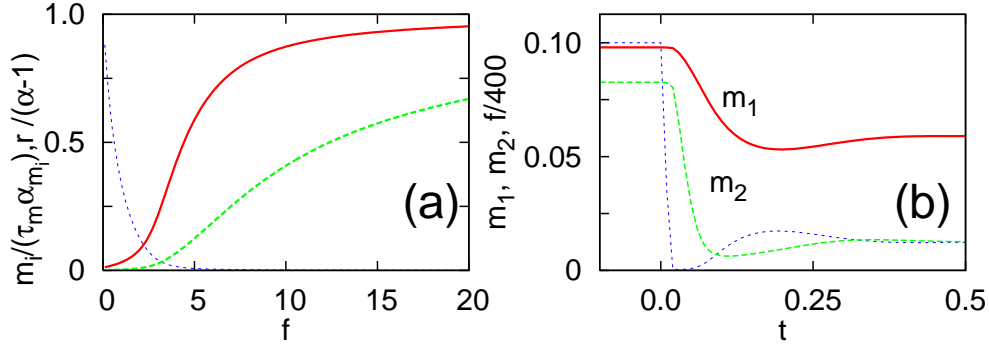


Figure 5. Investigation of mRNA prioritization by the sRNA motif. (a) The steady state level of $r/(\alpha-1)$ (blue dotted line), $m_1/(\tau_m \alpha_{m_1})$ (red solid line), and $m_2/(\tau_m \alpha_{m_2})$ (green dashed line) vs. f for $\alpha = 4$, $\gamma_1 = 150$, and $\gamma_2 = 1500$. (b) The time evolution of f (divided by 400, blue dotted line), m_1 (red solid line), and m_2 (green dashed line) after the sudden drop of C at $t = 0$.

The prioritization behavior is easily understood by considering the extreme case where both γ s are very large but $\gamma_2 \gg \gamma_1$. Then, depending on the level of f , the steady state is such that either (i) both mRNAs are near-zero, (ii) only m_1 is non-zero, (iii) both m_1 and m_2 are non-zero.

Taking into account finite γ values, the prioritization efficiency becomes, respectively,

- (i) $m_1 \approx O(1/\gamma_1)$ and $m_2 \approx O(1/\gamma_2)$ for small f , i.e. $f \lesssim \frac{\alpha}{\alpha_{m_1} + \alpha_{m_2}} - 1$,
- (ii) $m_1 \approx \tau_m(\alpha_{m_1} + \alpha_{m_2} - \frac{\alpha}{1+f})$ and $m_2 \approx O(\gamma_1/\gamma_2)$ for intermediate f , i.e. $\frac{\alpha}{\alpha_{m_1} + \alpha_{m_2}} - 1 \lesssim f \lesssim \frac{\alpha}{\alpha_{m_2}} - 1$,
- (iii) $m_1 \approx \tau_m \alpha_{m_1}$ and $m_2 \approx \tau_m(\alpha_{m_2} - \frac{\alpha}{1+f})$ for large f , i.e. $\frac{\alpha}{\alpha_{m_2}} - 1 \lesssim f$.

where the $O(x)$ are some functions that are small and proportional to x for small x .

Case (ii) is what we refer to as the “prioritized state”, where only one of the mRNA (the one with smaller γ) is present and the other’s level drops to near-zero. Clearly, the larger the difference between the γ values of the mRNAs, the better the prioritization; the order of magnitude difference in γ is important to have the clear prioritization. In addition, α , the sRNA production rate, determines the range of f for which the sRNA is affected, and a larger α results in prioritization being effective for a wider range of f .

In addition, the dynamics in Figure 5b shows that, when C is suddenly dropped, the mRNA with a larger γ value is rapidly depleted while the other mRNA stays at a higher level. That is, the sRNA is not only able to prioritize the mRNA steady state levels, but is also able to remove the “unwanted” mRNA m_2 much quicker than the “wanted” mRNA m_1 .

3.3.2. Prioritization of multiple mRNAs It is clear that the prioritization can be generalized to the case of more than two kinds of mRNAs regulated by a single type

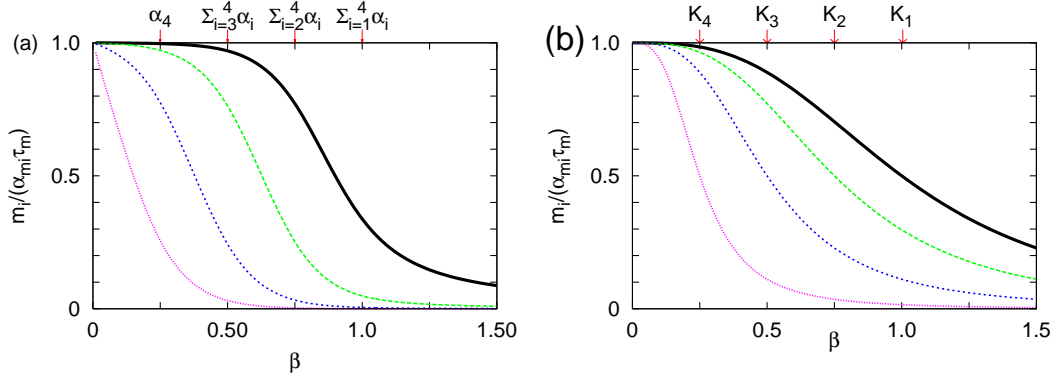


Figure 6. Prioritization of mRNAs by (a) sRNA regulation and (b) transcriptional regulation. The steady state level of mRNAs normalized by their maximum value is plotted against β . (a) The prioritization by sRNA regulation, for $\alpha_{m_1} = \alpha_{m_2} = \alpha_{m_3} = \alpha_{m_4} = 0.25$, and $\gamma_1 = 10^2, \gamma_2 = 10^3, \gamma_3 = 10^4, \gamma_4 = 10^5$. The value of γ_i are chosen to be large and have 10-fold difference between different mRNAs, so that the separation becomes clear. (b) Transcriptional regulation, where the transcription factor has concentration β and acts as a repressor. The Hill coefficient h is 3. The binding constants are $K_1 = 1, K_2 = 0.75, K_3 = 0.5$, and $K_4 = 0.25$. The values of K_i are chosen to be $K_i = \sum_{j=i}^4 \alpha_{m_j}$, so that the value of β at which the mRNA starts to be significantly degraded is the same for the two motifs.

of sRNA. To illustrate this we ignore feedback through f and consider the following general system with n different types of mRNAs:

$$\frac{dr}{dt} = \beta - r - \sum_{i=1}^n \gamma_i r m_i, \quad (11)$$

$$\frac{dm_i}{dt} = \alpha_{m_i} - \frac{m_i}{\tau_m} - \gamma_i r m_i \quad \text{for } i = 1, n. \quad (12)$$

Here, to focus on the prioritization, the production term of sRNA in (8) which contains feedback from iron concentration is replaced by a constant β . We assume $\gamma_1 < \gamma_2 < \dots < \gamma_i < \gamma_{i+1} < \dots < \gamma_n$ without loss of generality, and rescale all variables to be dimensionless such that $\sum_{i=1}^n \alpha_{m_i}$ and the degradation time of sRNA are unity.

Figure 6a shows the normalized steady state level of mRNAs, $m_i / (\alpha_{m_i} \tau_m)$, versus the production rate of the sRNA, β . As β becomes larger, sRNA increases and more mRNAs are degraded. As shown in Figure 6a, the n -th mRNA with the largest γ is degraded first. This also “protects” other mRNAs from degradation because the sRNAs are also degraded together with the n -th mRNAs. The $(n-1)$ -th mRNA starts to be degraded when the level of n -th mRNA becomes low enough, which occurs roughly at $\beta \approx \alpha_n$. The $(n-2)$ -th mRNA starts to be degraded when $\beta \approx \alpha_n + \alpha_{n-1}$, and so on, and finally all the mRNAs are almost completely degraded when $\beta \approx \sum_{i=1}^n \alpha_{m_i} = 1$. The separation of the level between the $(k+1)$ -th mRNA and the k -th mRNA for $\sum_{i=k+1}^n \alpha_{m_i} < \beta < \sum_{i=k}^n \alpha_{m_i}$ becomes clearer for larger difference between γ_{i+1} and γ_i .[§] This multistep-switch-like degradation upon changing the value

§ In the case $\gamma_{i+1}/\gamma_i \ll 1$ for any i , the steady state level of mRNA for $\sum_{i=k+1}^n \alpha_{m_i} < \beta < \sum_{i=k}^n \alpha_{m_i}$

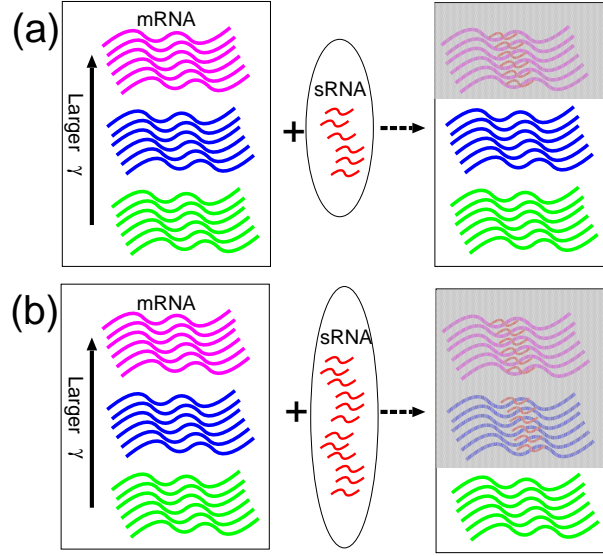


Figure 7. Schematic picture of the prioritization of various kinds of mRNAs by a single type of sRNA. Different kinds of mRNAs are represented by different colors, and have different value of γ (left boxes). (a) When a small amount of sRNAs is produced, the mRNAs with larger γ are degraded (shaded region in the right box), while the levels of mRNAs with small γ are scarcely affected. (b) As more sRNA is produced, the mRNAs with smaller γ are also degraded.

of β is the characteristic feature of the sRNA regulation. This prioritization mechanism is schematically presented in Figure 7, where the mRNAs are degraded in descending order of the value of γ .

We note that it is possible to have different steady state of mRNAs in the transcriptional motif also. Suppose r is the concentration of the repressor with a production rate β . Then the simplest model for the mRNA level is

$$\frac{dr}{dt} = \beta - r, \quad (13)$$

$$\frac{dm_i}{dt} = \frac{\alpha_{m_i}}{1 + (r/K_i)^h} - \frac{m_i}{\tau_m} \quad \text{for } i = 1, n. \quad (14)$$

with a Hill coefficient h and binding constants K_i ; we assume $K_1 > K_2 > \dots > K_n$ without loss of generality. Here, the variables are rescaled to be dimensionless such that K_1 and the degradation time of r are unity. The normalized steady state level is given by $m_i/(\alpha_{m_i}\tau_m) = \frac{1}{1+(\beta/K_i)^h}$: The levels decrease as β increases with the slope determined by the Hill coefficient h , and the characteristic value of β where the m_i level becomes half of its maximum is given by K_i . Figure 6b shows the separation of the steady state by transcription regulation with a relatively high value of the Hill coefficient $h = 3$ and various values of K_i . We see that the separation of the m_i level is not as sharp as with sRNA regulation, and m_i does not change much upon changing β especially for large

is estimated as follows: $m_i/(\tau_m\alpha_{m_i}) \approx 1$ for $i < k$, $m_k/(\tau_m\alpha_{m_k}) \approx (\sum_{i=k}^n \alpha_{m_i} - \beta)/\alpha_{m_k}$, and $m_i/(\tau_m\alpha_{m_i}) \ll 1$ for $i \geq k + 1$.

K_i . The sRNA regulation is more effective in the sense that the prioritization of the mRNAs is sensitive to small changes in β .

4. Discussion

Our analysis pinpoints three features that are particular to sRNA regulation in a feedback system. First, as sRNAs act through degradation, the regulation can, in principle, be very fast, generating a near instant response. Second, as the sRNA motif uses a double negative link, instead of a direct activation regulation, it has a higher metabolic cost for conditions where downstream targets are repressed. Third, and most interestingly, it has the capability of efficiently prioritizing the usage of downstream target genes.

It is essential for the prioritized expression of downstream targets that the sRNA as well as the mRNAs are degraded together after they form a complex. In the large γ limit, the effective prioritization occurs because the degradation of m_2 interferes with the degradation of m_1 by sequestering r , leaving less unbound r to bind m_1 . Indeed, if the sRNA simply catalyzed the degradation of the mRNAs without itself being degraded (i.e., no $\gamma_i m_i$ terms in (8) or (11)), the “protection” of m_1 is also lost. The degradation of different mRNAs doesn’t interfere as in the previous case, and thus the prioritization is less effective.

The switch-like behavior due to the “ultrasensitivity” of the sRNA regulation [4] together with the prioritization suggested in this work opens the possibility of more sophisticated regulation of gene expression. In particular, if each mRNA is targeted by several kinds of sRNAs, the combinatorics allows one to realize various logic gates. For example, if different kinds of sRNAs can bind to the same part of the targeted mRNA to trigger the regulation, it behaves as an “OR” gate. Such an example is known in *V. cholerae*, where four different sRNAs regulate HapR and any one of them is enough for regulation[4]. It is also, in principle, possible that one mRNA has multiple binding sites for different sRNAs ||. In this case, if binding of all the sRNAs is necessary to trigger the regulation, it realizes an “AND” gate. The concentration dependent prioritization can add more complicated functions to the logic gates. It is an interesting future issue to explore the possibility of combinatoric regulation by sRNAs.

We have tested numerically that the results of this paper do not strongly depend on the specific form of (3) for f . As long as in- and out-fluxes are large enough to allow a much faster response of f than of m , then m is the rate-limiting factor. Another thing to note is that we assumed that the Hill coefficient for the repression of sRNA by f is 1, though we introduced a Hill coefficient $h = 3$ in the transcription motif to achieve the sharp contrast in m at high and low f . If we put a Hill coefficient $H > 1$ in the sRNA motif by replacing the production term of r with $\alpha/(1 + f^H)$, the m vs. f curve becomes even steeper, which makes the response sharper.

|| The authors do not know of an established example, but there exists an mRNA that has multiple binding sites for the same micro RNA in eukaryotic cells [15, 16]

5. Experimental tests

The suggested prioritization possibility for downstream mRNAs invites experimental tests. One key quantity of interest is the degradation parameter γ , which in fact sets the efficiency of the whole sRNA regulatory system. For large γ , the sRNA regulation works as a step function: when production of sRNA is larger than production of downstream targets, these are instantly removed. Therefore it is essential to measure degradation times of downstream targets under various expression levels of the sRNA. These degradation times are tightly coupled to the steady state level of downstream mRNA, and could therefore be obtained from bulk measurements, using for example microarrays for both RyhB and downstream targets. For a given r (=sRNA) in the steady state, the downstream mRNA level is $m_i(r) = \alpha_{m_i}/(1/\tau_m + \gamma_i r)$, and therefore the slope of $m_i(0)/m_i(r) - 1$ versus r gives $\gamma_i \tau_m$.

An experimental test of the prioritization capability of the RyhB system is to consider homeostasis, and compare wild type with any mutant where the RyhB binding part of a downstream target gene is highly over-expressed. The over-expressed genes should be constructed such that they do not produce proteins that can bind Fe, and thereby indirectly influence the free/loosely bound Fe pool. For a given low level of external iron, the prioritized usage implies that for mutants where the over-expressed gene has small γ the expression levels of other genes would be almost the same as in wild type. For the remaining, there will be large changes associated to RyhB being depleted by the over-expressed gene with large γ . If the difference in γ between different target mRNA is of an order of magnitude, i.e., enough to have clear prioritization, the influence of the over-expressed gene should be quite sharp. Further, our prioritization scheme implies that as the external Fe is depleted further, the number of downstream genes which influence homeostasis should diminish monotonically.

6. Conclusion

Using the well characterized homeostatic response system for iron in bacteria, we analyzed the pros and cons of sRNA versus transcription regulation. The investigated negative feedback motif of $\text{Fe} \rightarrow \text{FeFur} \rightarrow \text{proteins} \rightarrow \text{Fe}$ brings out the functional similarities and differences between the two alternative strategies of regulating downstream targets. For sufficiently high Hill coefficients, transcriptional regulation can reproduce the same steady state behavior as the sRNA regulation. Further, both regulations can in principle provide a fast response to sudden decreases in externally available iron. However, their functional capabilities differ in two important aspects.

- First, adjusting parameters to obtain similar response times, the sRNA motif results in more turnover of target mRNAs in iron-poor conditions, whereas the transcription motif results in more turnover in iron-rich conditions.
- Second, the sRNA allows a prioritization of expression level of downstream targets, thus efficiently regulating the usage of a limiting iron resource. At the same time,

unwanted mRNA is degraded more rapidly. This observation fits with the fact that the transcription motif is found in *H. pylori*, a bacterium with a small genome and limited capacity for genome regulation, while *E. coli*, which has a larger genome and can benefit from fine tuning of mRNA levels, has an sRNA motif.

Our analysis suggests new ways to analyze other systems where multiple sRNAs regulate a more complicated response, including for example quorum sensing [4]. There, mutual binding inhibition between the sRNAs and a central regulator (LuxR mRNA in *V. harveyi* [4], HapR mRNA in *V. cholerae* [17], and the translational regulator RsmA in *Pseudomonas* [18]), may allow signals from adhesion and host factors to differentiate the sRNAs and thereby their downstream targets. Overall, our analysis suggests that sRNAs or micro RNAs may allow a near-digital reorganization of cellular composition, an observation which concurs with their ubiquity in regulatory processes associated with development.

Acknowledgments

This work was funded by the Danish National Research Foundation. NM thanks the Yamada Science Foundation for supporting her stay at the NBI. SS is grateful for the Janos Bolyai Research Fellowship of the Hungarian Academy of Sciences.

Appendix: Parameters in the flux equation

We set the parameters A , B and C in eq. (3) using data on the uptake and usage of Fe in *E. coli* and *H. pylori*. These systems are characterized by a huge flux of free Fe^{++} , where the fluxes C , A and B are so large that the pool is replenished about 100 times per cell generation.

In more detail, the constant incoming flux, C , is partitioned into two channels, A and B, that are motivated by the two separate ways of using iron in the Fe-Fur system. Flow through channel A is regulated, i.e., it can be reduced during iron-starvation, and is proportional to the mRNA level, but independent of f when there is any substantial amount of f in the system [9]¶. In contrast, flow through channel B is proportional to f . In the case of the full Fe-Fur system [9] the regulation of this flux by other proteins becomes important when extracellular iron increases suddenly, but here we focus on the regulation by sRNA and therefore keep flow through channel B unregulated. That is, our motif is designed to respond to depletion of f . Our “minimal” motif cannot do without this B channel because removing it results in robust oscillations, for which there is no evidence in *E. coli* [5].

¶ When we simulate eq.(3), we used the form $df/dt = C - A \cdot m \cdot [f/(f + K_{cut})] - B \cdot f$ with $K_{cut} = 0.1$ to avoid the numerical difficulty due to the singularity at $f = 0$. This expression agrees with eq.(3) in the limit of $K_{cut} \rightarrow 0$.

The parameters in (3) are set as follows [9]: For conditions where extracellular iron is plentiful, we demand that the internal Fe^{++} level is such that $f = 40$ [9] in steady state, while at the same time the net in- and out-flux per cell generation is approximately 100 times larger, representing the fast turnover and high usage of Fe [5, 9]. In addition, we assume that the iron flux is equally partitioned between the A and B channels, because we found it best fulfills the homeostatic requirements in our full model [9]. These conditions set the value of two parameters $C = 4572$ (i.e. $C = 114 \times f$ [9]) and $B = 57$. The value of A is completely determined by the steady state level of m , which depends on the parameters in the regulation part of the motif (i.e., α and γ in the sRNA motif, or D and K_t in the transcription motif). For iron-starvation we demand that $f = 5$ [9], keeping the value of B and A constant. This condition is achieved by reducing C , reflecting the reduction in extracellular iron. The C change needed to get $f = 5$ is dependent on the values of the regulation part of the motif. Note that, for a given regulatory motif, the steady state value of f is a unique function of the influx C .

References

- [1] Gottesman S 2004 The small rna regulators of escherichia coli: roles and mechanisms. *Annu. Rev. Microbiol.*, **58** 303–328.
- [2] Farh K K, Grimson A, Jan C, Lewis B P, Johnston W K, Lim L P, Burge C B, and Bartel D P 2005 The widespread impact of mammalian micrnas on mRNA repression and evolution. *Science*, **310** 1817–1821.
- [3] Jones-Rhoades M W, Bartel D P, and Bartel B 2006 Micrnas and their regulatory roles in plants. *Annu. Rev. Plant Biol.*, **57** 19–53.
- [4] Lenz D H, Mok K C, Lilley B N, Kulkarni R V, Wingreen N S, and Bassler B L 2004 The small rna chaperone Hfq and multiple small rnas control quorum sensing in *Vibrio harveyi* and *Vibrio cholerae*. *Cell*, **118** 69–82.
- [5] Andrews S C, Robinson A K, and Rodriguez-Quinones F 2003 Bacterial iron homeostasis. *FEMS Microbiol. Rev.*, **27** 215–237.
- [6] Massé E and Arguin M 2005 Ironing out the problems: new mechanisms of iron homeostasis. *Trends Biochem. Sci.*, **30** 462–468.
- [7] Nunoshiba T, Obata F, Boss A C, Oikawa S, Mori T, Kawanishi S, and Yamamoto K 1999 Role of iron and superoxide for generation of hydroxyl radical, oxidative DNA lesions and mutagenesis in *Escherichia coli*. *J. Biol. Chem.*, **274** 34832–34837.
- [8] Keyer K and Imlay J A 1996 Superoxide accelerates dna damage by elevating free-iron levels. *Proc. Natl. Acad. Sci. (USA)*, **93** 13635–13640.
- [9] Semsey A, Andersson A M C, Krishna S, Jensen M H, Massé E, and Sneppen K 2006 Genetic regulation of fluxes: Iron homeostasis of escherichia coli,. *Nucl. Acids Res.*, **34** 4960–496.
- [10] Massé E and S. Gottesman S 2002 A small RNA regulates the expression of genes involved in iron metabolism in *Escherichia coli*. *Proc. Natl. Acad. Sci. (USA)*, **99** 4620–4625.
- [11] Massé E, Escorcia F E, and Gottesman S 2003 Coupled degradation of a small regulatory RNA and its mRNA targets in *Escherichia coli*. *Genes Dev.*, **17** 2374–2383.
- [12] Massé E, Vanderpool C K, and Gottesman S 2005 Effect of RyhB small RNA on global iron use in *Escherichia coli*. *J. Bacteriol.*, **187** 6962–6971.
- [13] Delany I, Spohn G, Rappuoli R, and Scarlato V 2001 The fur repressor controls transcription of iron-activated and -repressed genes in *H. pylori*. *Mol. Microbiol.*, **42** 1297–1309.
- [14] Danielli A, Roncarati D, Delany I, Chiini V, Rappuoli R, and Scarlato V 2006 In vivo dissection of

- the *Helicobacter pylori* Fur regulatory circuit by genome-wide location analysis. *J. Bacteriol.*, **188** 4654–4662.
- [15] Hobert O 2004 Common logic of transcription factor and microRNA action. *Trends in Biochem. Sci.*, **29** 462–468.
- [16] Chang S, Johnston Jr R J, Frokjaer-Jensen C, Lockery S, and Hobert O 2004 MicroRNAs act sequentially and asymmetrically to control chemosensory laterality in the nematode. *Nature*, **430** 785–789.
- [17] Jobling M G and Holmes R K 1997 Characterization of hapR, a positive regulator of the *Vibrio cholerae* HA/protease gene hap, and its identification as a functional homologue of the *Vibrio harveyi* luxR gene. *Mol. Microbiol.*, **26** 1023–1034.
- [18] Pessi G, Williams F, Hindle Z, Heurlier K, Holden M T G, Cara M, Haas D, and Williams P 2001 Global posttranscriptional regulator RsmA modulates production of virulence determinants and N-acylhomoserine lactones in *Pseudomonas aeruginosa*. *J. Bacteriol.*, **183** 6676–6683.